



OPEN

Near-infrared excitation Raman spectroscopy of colored fabric contaminated with body fluids

Isaac D. Juárez & Dmitry Kurouski✉

Confirmatory identification of dyes in the physical pieces of evidence, such as hair and fabric, is critically important in forensics. This information can be used to demonstrate the link between a person of interest and a crime scene. High performance liquid chromatography is broadly used for dye analysis. However, this technique is destructive and laborious. This problem can be overcome by near-Infrared excitation Raman spectroscopy (NIR-RS), non-invasive and non-destructive technique that can be used to determine chemical structure of highly fluorescent dyes. Analyzed fabric materials often possess body fluid stains, which may obscure the accuracy of NIR-RS-based identification of dyes. In this study, we investigate the extent to which fabric contamination with body fluids can alter the accuracy of NIR-RS. Our results showed that NIR-RS coupled with partial-least squared discriminant analysis (PLS-DA) enabled on average 97.6% accurate identification of dyes on fabric contaminated with dry blood, urine and semen. We also found that NIR-RS could be used to identify blood, urine and semen on such fabric with 99.4% accuracy. Furthermore, NIR-RS could be used to differentiate between wet and dry blood, as well as reveal the presence of blood on washed fabric. These results indicate that NIR-RS coupled with PLS-DA could be used as a robust and reliable analytical approach in forensic analysis of fabric.

Forensic examination of fabric found at a crime scene is critically important in forensics^{1,2}. Such analysis could be used to reveal the chemical nature of the fabric material, its colorant composition, as well as the presence of biological and non-biological contaminants. All this information can help to establish a connection between a suspect and the crime scene.

Fluorescence, Infrared (IR) and Raman spectroscopy (RS) are broadly used to determine the chemical structure and composition of analyzed forensic samples, including fabric and body fluids^{3–11}. These techniques can easily differentiate between synthetic and natural fibers. At the same time, the accuracy of these techniques could be lowered by contaminants present in the fabric. High-performance liquid chromatography and mass-spectroscopy are commonly used to analyze dye composition of fabric¹². Although highly accurate, these analytical methods are laborious, invasive and destructive¹³. They also require an extensive library of colorants for the confirmatory identification of dyes. A large number of techniques ranging from optical microscopy to vibrational spectroscopy could reveal the presence of biological and non-biological contaminants on fabric^{14–16}. For instance, RS is capable of differentiating between blood, saliva, sweat, and semen^{17–20}. Furthermore, RS could be used to determine the age of bloodstains on different substrates²¹. Hager and co-workers showed that RS was capable of identifying urine on a large variety of fabric ranging from cotton to synthetic polyester⁶. Although this method is non-invasive and non-destructive, RS is limited to substrates with low fluorescence background²². At the same time, dyes of plant and insect origin that are broadly used for fabric coloration typically have extremely high fluorescence background, which limits the application of traditional RS for their analysis²³.

The problem of dye fluorescence can be overcome by the use of plasmonic nanostructures that enhance Raman scattering^{24–26}. This analytical approach, known as surface-enhanced Raman spectroscopy (SERS), is broadly used for the confirmatory identification of hair colorants in the artwork^{12,23,27,28}. SERS is also capable of detecting explosives^{29,30}, illicit drugs, such as heroin and cocaine³¹, and body fluids on fabric³². Furthermore, SERS could be used to detect and identify dyes present on hair^{33–36}.

Recently, our group demonstrated that fabric dyes could be identified using near-Infrared excitation Raman spectroscopy (NIR-RS)³⁷. In this case, utilization of near-Infrared lasers allows for the minimization of dye fluorescence, while preserving the entirely non-invasive and non-destructive nature of RS. Specifically, we found that

Department of Biochemistry and Biophysics, Texas A&M University, College Station, TX 77843, USA. ✉ email: dkurouski@tamu.edu

15 different colorants could be identified on cotton fabric with ~ 100% accuracy with only 1 s spectral acquisition using a hand-held NIeRS³⁷.

It should be noted that physical pieces of evidence found at crime scenes are typically exposed to a large number of substances of biological and non-biological origin^{38,39}. Substances of the first category typically include blood, semen, and urine. Substantially large variability is expected for the substances of non-biological origin that can be present on fabric. These substances range from household and food contaminants to industrial products. Previously reported results by Juarez and Kuroski showed that the presence of blood on colored hair limits the use of SERS for the identification of artificial hair dyes^{38,39}. Similar conclusions were made for a large number of household contaminants^{38,39}. However, if removed by washing, the information about the hair colorants could be revealed by SERS.

Expanding upon this, we investigated the extent to which blood, semen and urine could alter the accuracy of NIeRS-based analysis of green, pink, and light red dyes on cotton fabric. We also investigated the extent to which body fluids could be identified using NIeRS on blank and colored cotton fabric. For this, partial least-squared discriminant analysis (PLS-DA) was used. In general, PLS-DA performs the same or better than support vector machine (SVM), soft independent modeling of class analogy (SIMCA), and principal component analysis (PCA)^{40,41}. This method integrates regression and classification by leveraging the correlation between spectral data and sample classes. Unlike binary classifiers such as SVM and SIMCA, PLS-DA is capable of handling multiclass classification, making it more suitable for complex classification tasks. Furthermore, unlike PCA, which only identifies the most significant components in the data, PLS-DA extracts latent variables that optimize the correlation between spectral datapoints and class variables, thus enhancing its performance in datasets with intricate class structures and small sample sizes.

Experimental section

Fabric materials

Cotton canvas was purchased from Fruit of the Loom; green, pink and light red dyes (Kool Krafts, ASIN: B08N5HVXS8) were purchased from the Mosaiz Store (Vanstek Tie Dye Kit, 24 Colors Tie Dye Shirt DIY Fabric Dyes). These non-reactive colorants became highly popular around the world and broadly used to dye fabric. Coloration was performed by soaking the cotton in the corresponding liquid dye for 1 h. Next, cotton samples were rinsed under cold water until the water ran clear and dried under ambient conditions.

Near-infrared excitation Raman spectroscopy (NIeRS)

NIeRS spectra were collected using a hand-held Agilent Resolve spectrometer equipped with an 830 nm laser. Spectra were acquired with 1 s acquisition time and 495 mW laser power. Automatic baselining was performed by the instrument. Spectra were taken at different locations on the fabric sample.

Spectral processing and statistical analysis

Spectral processing and model development was done in Matlab (Mathworks) equipped with PLS_Toolbox (Eigenvector Research, Inc., Manson, WA).

Results and discussion

We first used NIeRS to examine vibrational fingerprints of dyes themselves on cotton fabric. For this, blank pieces of cotton were colored by green, light red and pink dyes. Acquired NIeRS spectra revealed vibrational fingerprints that were unique to all three colorants, Fig. 1. We found that green colorant could be identified by the presence of 750 and 1540 cm^{-1} , whereas light red dye exhibited a unique vibrational band at 1412 cm^{-1} . Pink colorant has two unique vibrational bands at 1285 and 1610 cm^{-1} .

It should be noted that although some colorants have only one unique band, utilization of partial-least squared discriminant analysis (PLS-DA), allowed for the highly accurate identification of all three colorants on fabric, Table 1 and Figure S1–S2.

Next, undyed cotton fabric was contaminated with blood, urine and semen and dried under room temperature. Visual examination of samples revealed intense-brown and light-yellow coloration of blood- and urine-contaminated samples, respectively, Fig. 2A–C. No visual change in the color of semen-contaminated sample was observed, Fig. 2D.

NIeRS-based analysis of the contaminated uncolored fabric revealed a strong signature of heme and proteins in the spectrum acquired from the blood-contaminated fabric. Specifically, we observed an increase in the intensity of 730–750 cm^{-1} bands (aromatics), 1236 cm^{-1} (amide III) and 1455 cm^{-1} (CH_2), as well as 1555–1618 cm^{-1} , which could be assigned to amide II and I bands on proteins, Fig. 2E. These results indicate that NIeRS could be used to detect the presence of blood on fabric. We also observed an increase in the intensity of 1000 cm^{-1} band in the NIeRS spectrum acquired from urine-contaminated fabric compared to NIeRS spectrum of clean fabric. Hager and co-workers previously showed that this band originates from urea⁶. Finally, only minor changes in the intensities of vibrational bands were observed in NIeRS spectrum of blank fabric with dried semen contamination. These results indicate that semen does not have strong spectroscopic signature if present on fabric that could be used for its unambiguous identification. It should be noted that 1000 cm^{-1} band was also observed in NIeRS spectra acquired from fabric contaminated by blood. In this case, this band originates from aromatic vibrations of proteins. However, in the case of blood, another vibrational bands that correspond to heme and proteins were observed. Thus, 1000 cm^{-1} alone cannot be solely used to differentiate between the presence of blood vs urine.

We also investigated the extent to which spectroscopic signatures of blood on undyed cotton could be altered if the body fluid was not dried and if it was removed by washing. As expected, the presence of fresh blood can be noticed by the naked eye on uncontaminated cotton, Fig. 3A. However, extensive washing of the cotton material

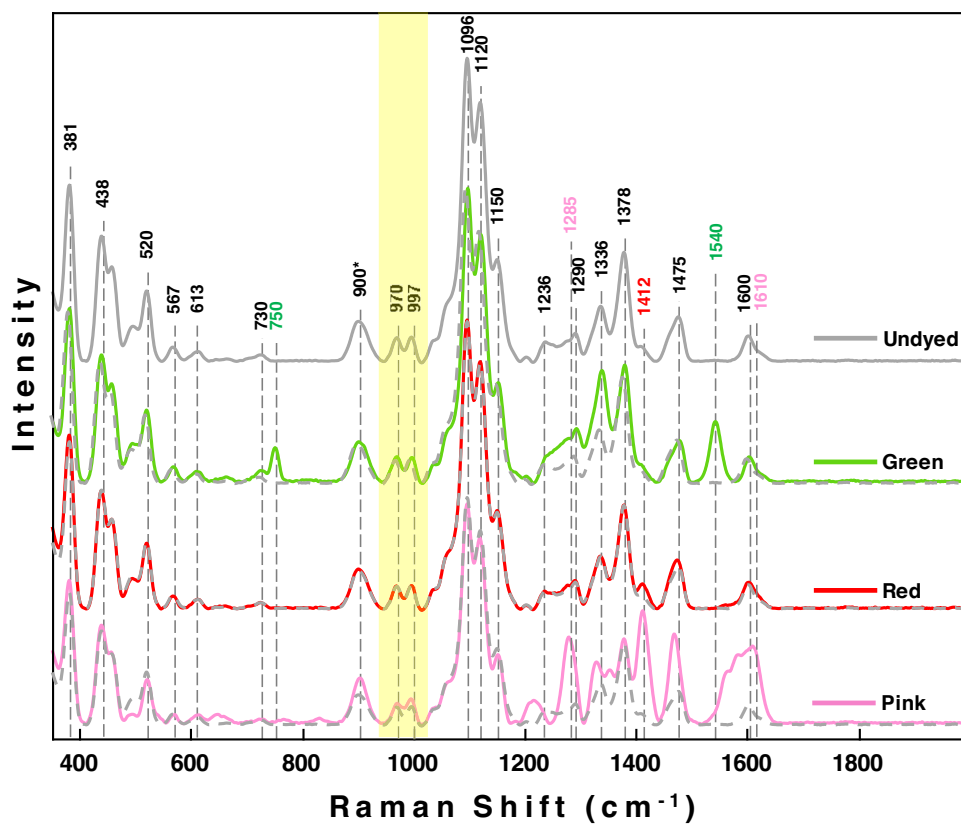


Figure 1. NIeRS spectra of undyed (grey), green-, light red-, and pink-colored fabric with corresponding undyed spectra shown next to each. Differences between intensities of 970 and 997 cm^{-1} are highlighted by a yellow bar.

| | Model 1 |
|----------------------|-------------------------------|
| Color | Internal Validation (N = 100) |
| True prediction rate | |
| Undyed | 100% |
| Green | 100% |
| Light Red | 96% |
| Pink | 100% |

Table 1. Confusion matrix of PLS-DA model with cross (internal) validation showing the accuracy of NIeRS-based identification of dyes on uncontaminated fabric.

with detergents did not allow for the complete removal of the blood from the fabric. Clearly visible brown coloration was evident on such fabric, Fig. 3B.

We found that dried and wet blood have substantially different vibrational fingerprints on uncontaminated cotton. Specifically, we observed strong changes in 730–750, 1236 and 1455, 1555–1618 cm^{-1} , spectral regions, Fig. 3C. These results indicated that NIeRS could be used to reveal changes in composition of blood that take place upon drying. These results are consistent with experimental findings reported by Doty and co-workers⁴³. The researchers also showed that RS could be used to identify aging of bloodstains⁴³. Therefore, in our study, we analyzed blood dried only for 24 h. We also found very little if any difference in the spectroscopic signature of fabric after the blood was removed by drying. At the same time, PLS-DA allowed for unambiguous identification of all analyzed classes of samples, Fig. 4. Thus, NIeRS could be used to identify whether contaminated fabric was exposed to blood and if yes, whether blood was removed by washing, Table 2 and Figures S3 and S4.

Similar effects of body fluids were observed for green-, pink-, and light red-colored fabric. Specifically, the greatest magnitude of the spectroscopic changes was caused by blood in all three cases. Nearly all regions of the NIeRS spectra were altered by the presence of this body fluid. We also found that the presence of urine caused an increase in the intensity of 1000 cm^{-1} in the NIeRS spectra acquired from green, pink, and light red-colored

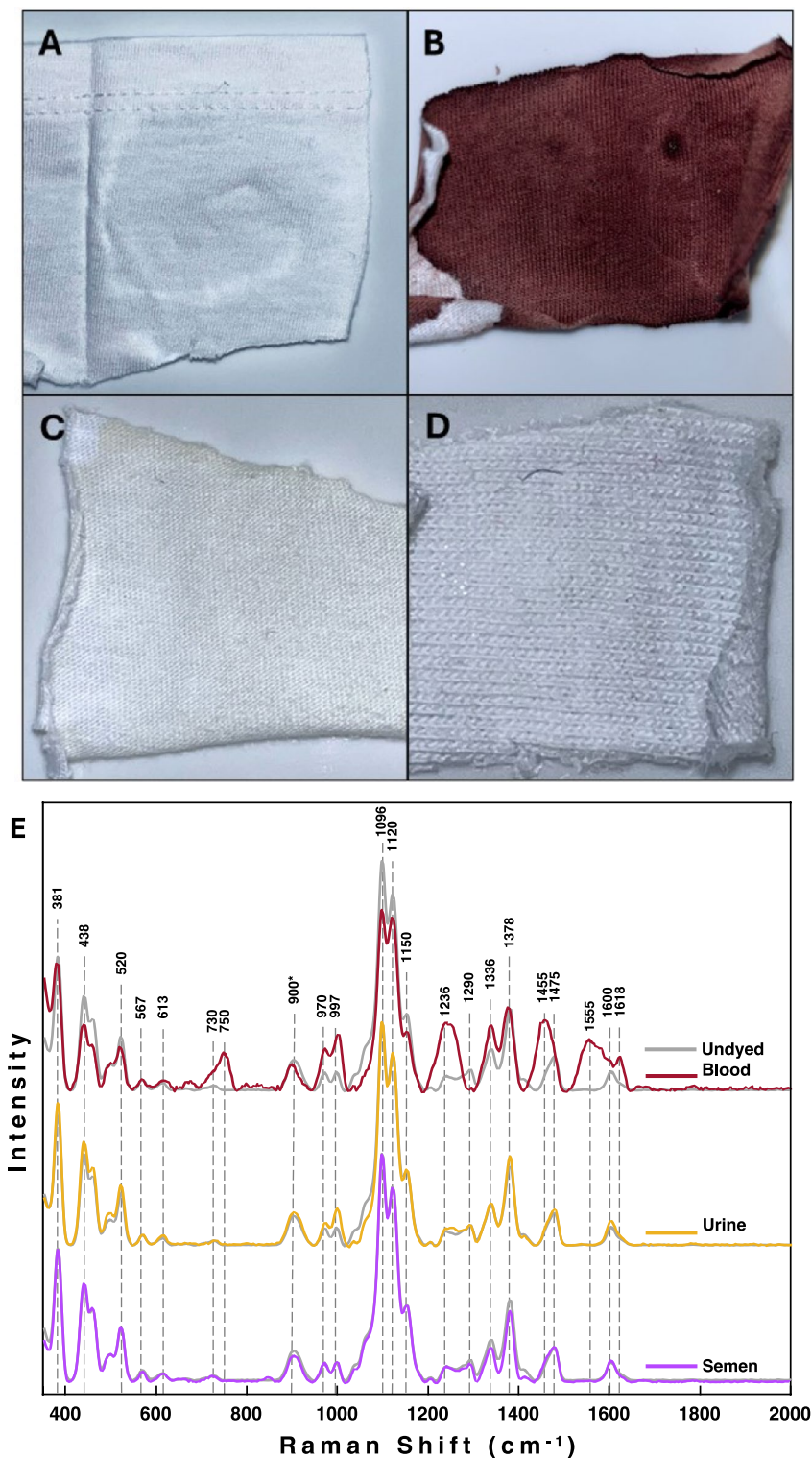


Figure 2. Photographs of uncontaminated (A) cotton fabric and the fabric contaminated with blood (B), urine (C) and semen (D). NIERS spectra (E) of blank (grey), fabric contaminated with blood (maroon), urine (yellow) and semen (pink) with corresponding blank spectra shown by dashed lines. Spectra were normalized on 900 cm⁻¹ indicated by an asterisk (*).

Finally, the presence of semen did not cause changes in any particular peak. However, similar to the uncolored fabric, primarily changes in the intensities of some vibrational bands were observed, Fig. 5.

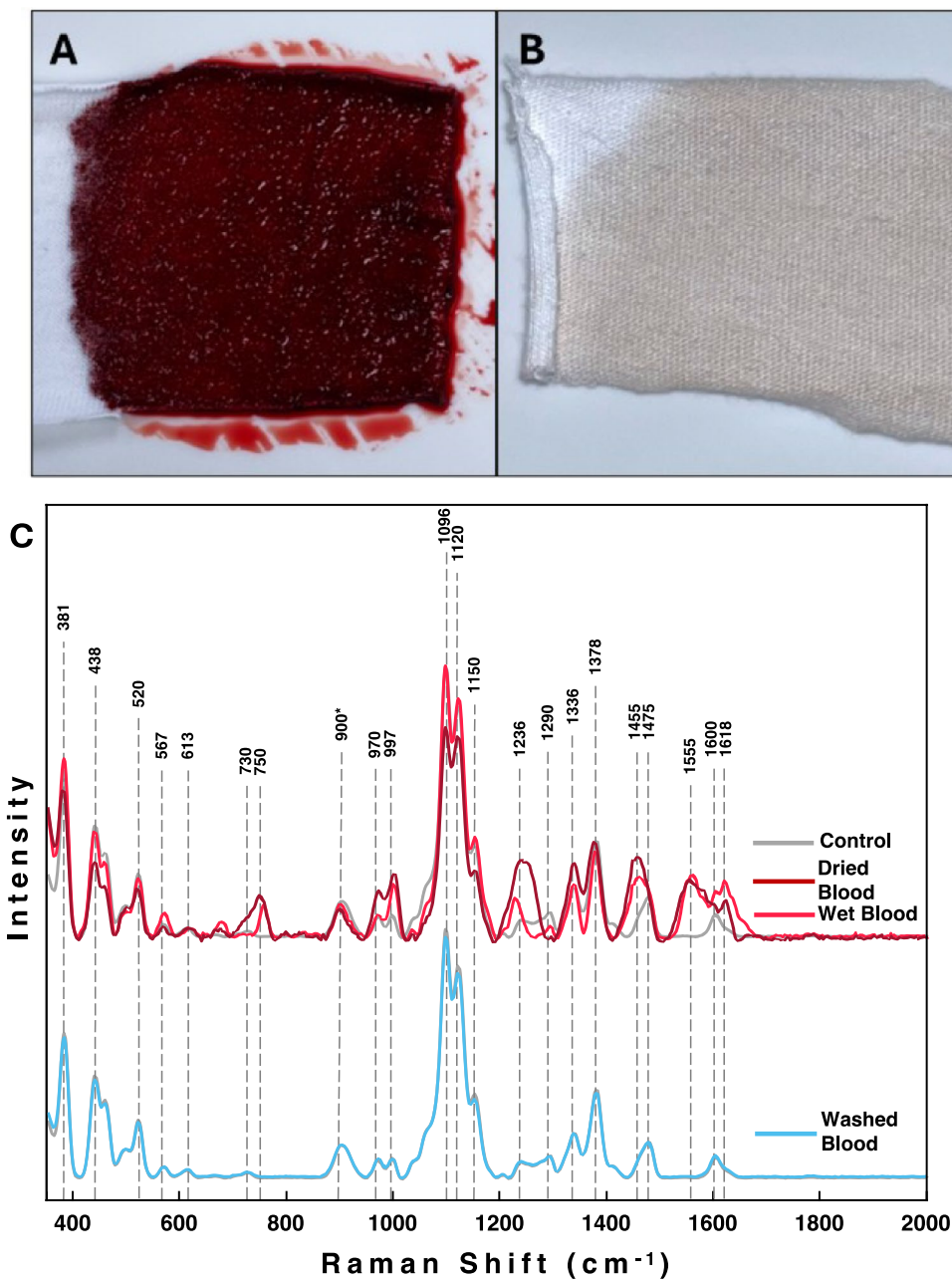


Figure 3. Photographs of cotton fabric exposed to fresh blood before (A) and after washing (B). NIERS spectra (C) acquired from wet and dried blood present on uncontaminated (control) fabric, as well as the spectra acquired from fabric after removal of blood by washing. Spectra were normalized on 900 cm^{-1} indicated by an asterisk (*).

Next, we investigated the extent to which artificial intelligence could be used to determine the color of fabric with and without present contaminants. For this, 16 classes of data were used, Scheme 1. We first built a PLS-DA model based on all 16 classes of data and used cross-validation to identify the accuracy of color identification. The second PLS-DA model was built on 11 classes of data (training model) with the remaining 5 classes used for external validation. Our results indicate that cross-validation enabled highly accurate identification of both green and pink dyes (100% accuracy), whereas uncolored fabric and light red fabric were identified with 96.7% and 92.8%, respectively. External validation of this model enabled 100% accurate identification of green and pink dyes, with 88% identification of the light red colorant, Table 3 and Figures S5–S7. These results indicate that NIERS could be used for highly accurate identification of colorants of the fabric with and without present contaminants. Furthermore, the design of the training model indicates that robust PLS-DA models for color identification are possible after only exposing the learning algorithm to the control, allowing the number of colors recognized to be easily upscaled.

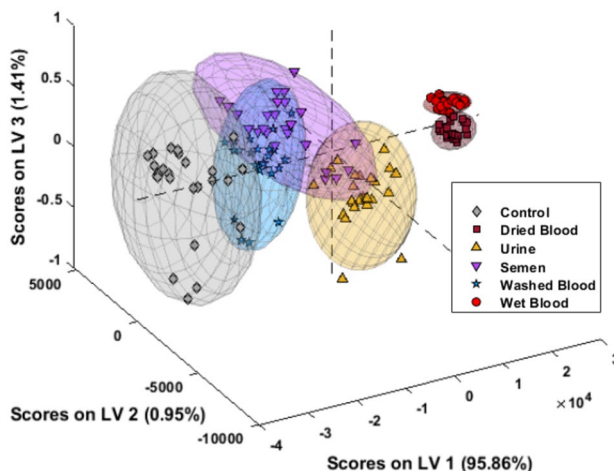


Figure 4. 3D latent-variable plot of NIRS spectra acquired from undyed cotton, as well as cotton contaminated by urine, semen, dry and wet blood.

| Textile Color | Actual Class, Internal Validation | | | | | | | |
|-----------------|-----------------------------------|----------------|------------------|--------------------|---------------------|-------|-------|---|
| | True Prediction Rate | Control (N=25) | Wet Blood (N=25) | Dried Blood (N=25) | Wash'd Blood (N=25) | Urine | Semen | |
| Predicted Class | | | | | | | | |
| Control | 96% | 24 | 0 | 0 | 0 | 0 | 0 | 0 |
| Wet Blood | 100% | 0 | 25 | 0 | 0 | 0 | 0 | 0 |
| Dried Blood | 100% | 0 | 0 | 25 | 0 | 0 | 0 | 0 |
| Wash'd Blood | 100% | 1 | 0 | 0 | 25 | 0 | 0 | 0 |
| Urine | 100% | 0 | 0 | 0 | 0 | 25 | 0 | 0 |
| Semen | 100% | 0 | 0 | 0 | 0 | 0 | 25 | 0 |

Table 2. Confusion matrix of PLS-DA model with cross (internal) validation showing the accuracy of NIRS-based identification of contaminants on blank fabric.

The next question to ask is whether NIRS coupled with PLS-DA could be used to identify the presence of contaminants on fabric. To answer this question, we built a PLS-DA model in which all data were partitioned 80:20, where 80% of the data were used to build the model and 20% of the data were used to perform external validation, Scheme 2.

Our results show that both urine and semen could be identified with 100% accuracy in the case of cross- and external validation, Table 4 and Figures S8–S10. We also found that blood could be correctly identified with 98.3% and 88.3% accuracy in cross- and external validation, respectively. Finally, the absence of any contamination could be confirmed with ~ 90% accuracy. Finally, we investigated the extent to which wet, dry and washed blood could be identified on fabric. Our results show that external validation enabled 100% accurate identification of wet, dried blood, and washed blood on both uncolored and colored fabric, Table 5 and Figures S11 and S12.

Conclusions

Our proof-of-principle results demonstrate high sensitivity of NIRS to body fluid contaminants. Specifically, NIRS could be used for highly accurate identification of dry blood, urine, and semen present on both dyed and undyed model fabric samples. These results are in good agreement with experimental findings previously reported by Lednev group for Raman-based sensing with 785 nm^{42–44}. Furthermore, NIRS could identify whether fabric was exposed to blood after its washing. We also showed that NIRS was capable of identifying color of fabric with and without present contaminants. These results indicate that NIRS coupled with PLS-DA can be used in forensics analysis of dyes and contaminants present on cotton fabric. It is important to note that a hand-held NIRS instrument requires ~ 2–3 mm² of fabric for the analysis. However, the extension of this approach to the confocal microscopes could be used to identify both colorants and contaminants on fragments (20–30 μm²) of individual fibers (Supplementary file). Finally, it is very important to extend NIRS sensing of colorants on synthetic fabric, as well as to test the contribution of environmental factors, such as UV radiation and heat, as well as substances of non-biological origin on the reliability of NIRS-based identification of colorants on fabric.

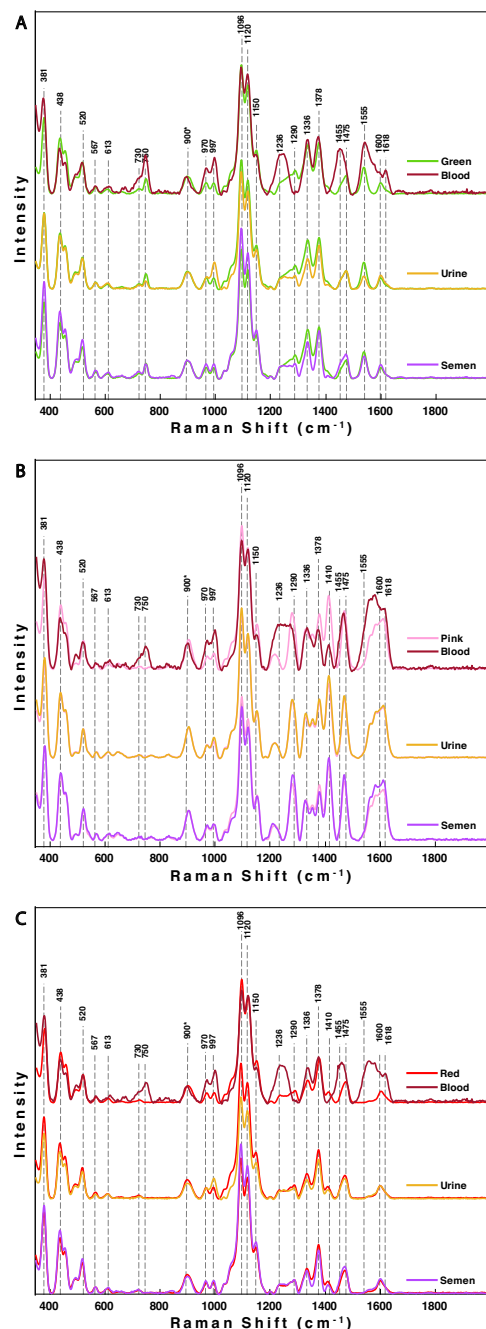
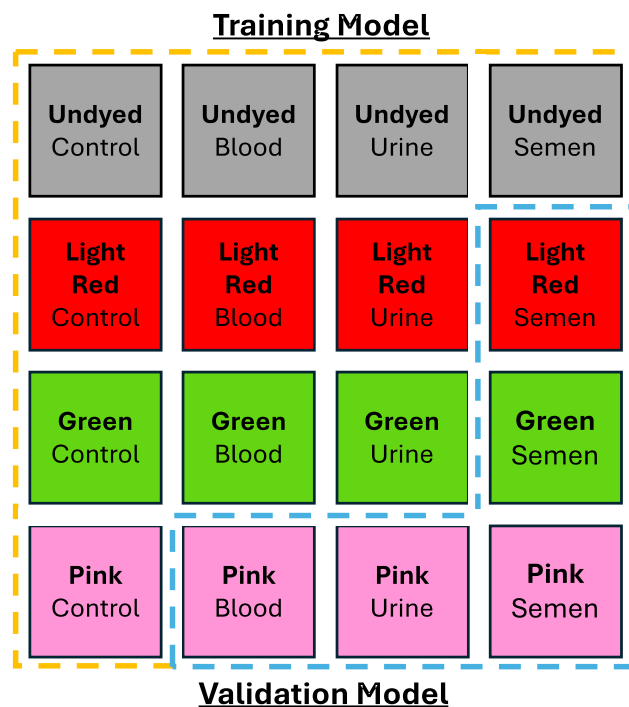


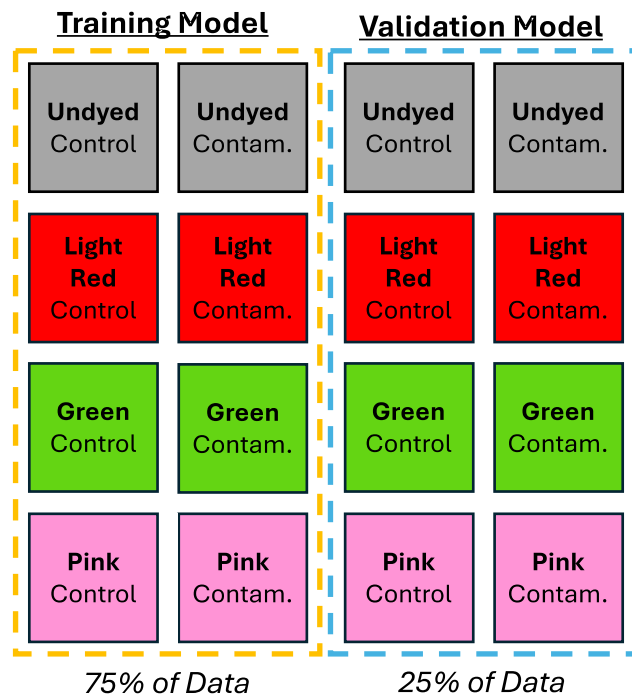
Figure 5. NIRS spectra of green (A), pink (B), and light red (C)-colored cotton fabric contaminated with blood, urine, and semen. Spectra were normalized on 900 cm⁻¹ indicated by an asterisk (*).



Scheme 1. Classes of data used for training and validation of PLS-DA model used to identify colorants on fabric.

| Actual Class, Internal Validation | | | | | | Actual Class, External Validation | | | |
|-----------------------------------|----------------------|-----------------|-----------------|---------------------|----------------|-----------------------------------|----------------|--------------------|---------------|
| Textile Color | True Prediction Rate | White (N = 150) | Green (N = 125) | Light Red (N = 125) | Pink (N = 125) | True Prediction Rate | Green (N = 25) | Light Red (N = 25) | Pink (N = 25) |
| Predicted class | | | | | | | | | |
| Undyed | 96.7% | 145 | 0 | 8 | 0 | N/A | 0 | 3 | 0 |
| Green | 100% | 1 | 125 | 1 | 0 | 100% | 25 | 0 | 0 |
| Light Red | 92.8% | 4 | 0 | 116 | 0 | 88% | 0 | 22 | 0 |
| Pink | 100% | 0 | 0 | 0 | 25 | 100% | 0 | 0 | 125 |

Table 3. Confusion matrix of PLS-DA model with cross (internal and external) validations showing the accuracy of NIERS-based identification of dyes on contaminated fabric.



Scheme 2. Classes of data used for training and validation of PLS-DA model used to identify body fluid contaminants.

| Model I | | |
|------------------------|-------------------------------|-------------------------------|
| Biological contaminant | Internal validation (N = 480) | External validation (N = 120) |
| True prediction rate | | |
| Control | 91.3% | 80% |
| Blood | 98.3% | 88.3% |
| Urine | 100% | 100% |
| Semen | 100% | 100% |

Table 4. Confusion matrix of PLS-DA model with cross (internal and external) validations showing the accuracy of NIERS-based identification of contaminants on fabric.

| | | Model II |
|------------------------|--|------------------------------|
| Biological Contaminant | | External Validation (N = 60) |
| True prediction rate | | |
| Wet Blood | | 100% |
| Dried Blood | | 100% |
| Washed Blood | | 100% |

Table 5. Confusion matrix of PLS-DA model with cross (external) validation showing the accuracy of NIERS-based identification between wet, dried and washed blood samples.

Data availability

The datasets used and/or analyzed during the current study available from the corresponding author on reasonable request.

Received: 27 April 2024; Accepted: 12 August 2024

Published online: 17 August 2024

References

1. Saferstein, R. Hairs, fibers, and paint. In *Criminalistics: An Introduction to Forensic Science*, 5th edn, 202–242 (Schuster, P.-H.-S. eds) (1995).
2. Robertson, J., Roux, C. & Wiggins, K. G. *Forensic Examination of Fibres* (CRC Press, Boca Raton, 2017).
3. Bueno, J. & Lednev, I. K. Attenuated total reflectance-FT-IR imaging for rapid and automated detection of gunshot residue. *Anal. Chem.* **86**(7), 3389–3396 (2014).
4. Bueno, J., Sikirzyhtski, V. & Lednev, I. K. Raman spectroscopic analysis of gunshot residue offering great potential for caliber differentiation. *Anal. Chem.* **84**(10), 4334–4339 (2012).
5. Edwards, H. G. M., Farwell, D. W. & Williams, A. C. FT-Raman spectrum of cotton: A polymeric biomolecular analysis. *Spectrochim. Acta A Mol. Spectrosc.* **50**(4), 807–811 (1994).
6. Hager, E., Farber, C. & Kurouski, D. Forensic identification of urine on cotton and polyester fabric with a hand-held Raman spectrometer. *Forensic Chem.* **9**, 44–49 (2018).
7. Weber, A. *et al.* Innovative vibrational spectroscopy research for forensic application. *Anal. Chem.* **95**(1), 167–205. <https://doi.org/10.1021/acs.analchem.2c05094> (2023).
8. Khandasamny, S. R. *et al.* Bloodstains, paintings, and drugs: Raman spectroscopy applications in forensic science. *Forensic Chem.* **8**, 111–133 (2018).
9. Biermann, T. Blocks of colour IV: The evidential value of blue and red cotton fibres. *Sci. Justice* **47**(2), 68–87 (2007).
10. Macrae, R., Dudley, R. & Smalldon, K. The characterization of dyestuffs on wool fibers with special reference to microspectrophotometry. *J. Forensic Sci.* **24**(1), 117–129 (1979).
11. Grieve, M. C., Dunlop, J. & Haddock, P. An investigation of known blue, red, and black dyes used in the coloration of cotton fibers. *J. Forensic Sci.* **35**(2), 301–315 (1990).
12. Casadio, F., Leona, M., Lombardi, J. R. & Van Duyne, R. Identification of organic colorants in fibers, paints, and glazes by surface enhanced Raman spectroscopy. *Acc. Chem. Res.* **43**(6), 782–791. <https://doi.org/10.1021/ar100019q> (2010).
13. Nacci, T., Sabatini, F., Cirrincione, C., Degano, I. & Colombini, M. P. Characterization of textile fibers by means of EGA-MS and Py-GC/MS. *J. Anal. Appl. Pyrolysis* **165**, 105570 (2022).
14. Luber, C. K., Doty, K. C., Bueno, J., Halamkova, L., & Lednev, I. K. Vibrational spectroscopy: Recent developments to revolutionize forensic science. *Anal. Chem.* (2014).
15. Cano-Trujillo, C., García-Ruiz, C., Ortega-Ojeda, F. E., Romolo, F. & Montalvo, G. Forensic analysis of biological fluid stains on substrates by spectroscopic approaches and chemometrics: A review. *Anal. Chim. Acta* **1282**, 341841. <https://doi.org/10.1016/j.aca.2023.341841> (2023).
16. Zapata, F., Ortega-Ojeda, F. E. & García-Ruiz, C. Forensic examination of textile fibres using Raman imaging and multivariate analysis. *Spectrochim. Acta Part A Mol. Biomol. Spectrosc.* **268**, 120695. <https://doi.org/10.1016/j.saa.2021.120695> (2022).
17. Virkler, K. & Lednev, I. K. Raman spectroscopic signature of blood and its potential application to forensic body fluid identification. *Anal. Bioanal. Chem.* **396**(1), 525–534 (2009).
18. Virkler, K. & Lednev, I. K. Analysis of body fluids for forensic purposes: From laboratory testing to non-destructive rapid confirmatory identification at a crime scene. *Forensic Sci. Int.* **188**(1–3), 1–17 (2009).
19. McLaughlin, G., Doty, K. C. & Lednev, I. K. Discrimination of human and animal blood traces via Raman spectroscopy. *Forensic Sci. Int.* **238**, 91–95 (2014).
20. Sikirzyhtskaya, A., Sikirzyhtski, V. & Lednev, I. K. Raman spectroscopy coupled with advanced statistics for differentiating menstrual and peripheral blood. *J. Biophoton.* **7**(12), 59–67 (2012).
21. Zhang, R., Wang, P., Chen, J., Tian, Y. & Gao, J. Age estimation of bloodstains based on Raman spectroscopy and chemometrics. *Spectrochim. Acta Part A Mol. Biomol. Spectrosc.* **290**, 122284. <https://doi.org/10.1016/j.saa.2022.122284> (2023).
22. Farber, C., Mahnke, M., Sanchez, L. & Kurouski, D. Advanced spectroscopic techniques for plant disease diagnostics. A review. *Trends Analyt. Chem.* **118**, 43–49 (2019).
23. Casadio, F., Daher, C. & Bellot-Gurlet, L. Raman spectroscopy of cultural heritage materials: Overview of applications and new frontiers in instrumentation, sampling modalities, and data processing. *Top. Curr. Chem. (Cham.)* **374**(5), 62. <https://doi.org/10.1007/s41061-016-0061-z> (2016).
24. Wustholz, K. L. *et al.* Structure–activity relationships in gold nanoparticle dimers and trimers for surface-enhanced Raman spectroscopy. *J. Am. Chem. Soc.* **132**(31), 10903–10910 (2010).
25. Zrimsek, A. B. *et al.* Single-molecule chemistry with surface- and tip-enhanced Raman spectroscopy. *Chem. Rev.* **117**(11), 7583–7613. <https://doi.org/10.1021/acs.chemrev.6b00552> (2017).
26. Sharma, B., Frontiera, R. R., Henry, A. I., Ringe, E. & Van Duyne, R. P. SERS: Materials, applications, and the future. *Mater. Today* **15**(1–2), 16–25 (2012).
27. Brosseau, C. L. *et al.* Ad-hoc surface-enhanced Raman spectroscopy methodologies for the detection of artist dyestuffs: Thin layer chromatography-surface enhanced Raman spectroscopy and in situ on the fiber analysis. *Anal. Chem.* **81**(8), 3056–3062. <https://doi.org/10.1021/ac802761v> (2009).
28. Idone, A. *et al.* Silver colloidal pastes for dye analysis of reference and historical textile fibers using direct, extractionless, non-hydrolysis surface-enhanced Raman spectroscopy. *Analyst* **138**(20), 5895–5903. <https://doi.org/10.1039/c3an00788j> (2013).
29. Riskin, M., Tel-Vered, R., Lioubashevski, O. & Willner, I. Ultrasensitive surface Plasmon resonance detection of trinitrotoluene by a Bis-aniline-cross-linked Au nanoparticles composite. *J. Am. Chem. Soc.* **131**(21), 7368–7378 (2009).
30. Sylvia, J. M., Janni, J. A., Klein, J. & Spencer, K. M. Surface-enhanced Raman detection of 2,4-dinitrotoluene impurity vapor as a marker to locate landmines. *Anal. Chem.* **72**(23), 5834–5840 (2000).
31. Wei, W. Y. & White, I. M. Inkjet-printed paper-based SERS dipsticks and swabs for trace chemical detection. *Analyst* **138**(4), 1020–1025 (2013).
32. Virkler, K. & Lednev, I. K. Raman spectroscopic signature of blood and its potential application to forensic body fluid identification. *Anal. Bioanal. Chem.* **396**(1), 525–534 (2010).
33. Holman, A. & Kurouski, D. The effects of sun exposure on colorant identification of permanently and semi-permanently dyed hair. *Sci. Rep.* **13**(1), 2168. <https://doi.org/10.1038/s41598-023-29221-8> (2023).
34. Holman, A. P. & Kurouski, D. Surface-enhanced Raman spectroscopy enables confirmatory detection of dyes on hair submerged in hypolimnion water for up to Twelve weeks. *J. Forensic Sci.* <https://doi.org/10.1111/1556-4029.15347> (2023).

35. Holman, A. P. & Kurouski, D. Role of race/ethnicity, sex, and age in surface-enhanced Raman spectroscopy- and infrared spectroscopy-based analysis of artificial colorants on hair. *ACS Omega* **8**(23), 20675–20683. <https://doi.org/10.1021/acsomega.3c01241> (2023).
36. Higgins, S. & Kurouski, D. Surface-enhanced Raman spectroscopy enables highly accurate identification of different brands, types and colors of hair dyes. *Talanta* **251**, 123762. <https://doi.org/10.1016/j.talanta.2022.123762> (2022).
37. Peterson, M. & Kurouski, D. Non-destructive identification of dyes on fabric using near-infrared Raman spectroscopy. *Molecules* **28**(23), 7864. <https://doi.org/10.3390/molecules28237864> (2023).
38. Juarez, I. & Kurouski, D. Surface-enhanced Raman spectroscopy hair analysis after household contamination. *Anal. Methods* <https://doi.org/10.1039/d3ay01219k> (2023).
39. Juarez, I. & Kurouski, D. Effects of crime scene contaminants on surface-enhanced Raman analysis of hair. *J. Forensic Sci.* **68**(1), 113–118. <https://doi.org/10.1111/1556-4029.15165> (2023).
40. Farber, C. & Kurouski, D. Raman spectroscopy and machine learning for Agricultural applications: Chemometric assessment of spectroscopic signatures of plants as the essential step toward digital farming. *Front. Plant Sci.* **13**, 887511. <https://doi.org/10.3389/fpls.2022.887511> (2022).
41. Shashilov, V. A. & Lednev, I. K. Advanced statistical and numerical methods for spectroscopic characterization of protein structural evolution. *Chem. Rev.* **110**(10), 5692–5713. <https://doi.org/10.1021/cr900152h> (2010).
42. Doty, K. C., Muro, C. K. & Lednev, I. K. Predicting the time of the crime: Bloodstain aging estimation for up to two years. *Forensic Chem.* **5**, 1–7 (2017).
43. McLaughlin, G., Fikiet, M. A., Ando, M., Hamaguchi, H. & Lednev, I. K. Universal detection of body fluid traces in situ with Raman hyperspectroscopy for forensic purposes: Evaluation of a new detection algorithm (HAMAND) using semen samples. *J. Raman Spectrosc.* **80**, 1147–1153 (2019).
44. Kistenev, Y. V., Borisov, A. V., Samarinova, A. A., Colon-Rodriguez, S. & Lednev, I. K. A novel Raman spectroscopic method for detecting traces of blood on an interfering substrate. *Sci. Rep.* **13**(1), 5384. <https://doi.org/10.1038/s41598-023-31918-9> (2023).

Acknowledgements

This project was supported by Award No. 2020-90663-TX-DU, awarded by the National Institute of Justice, Office of Justice Programs, U.S. Department of Justice.

Author contributions

I.J. collected and analyzed spectroscopic data. I.J. performed statistical analyses. I.J. and D.K. discussed results and wrote the manuscript. All authors approved of the final version of the manuscript.

Competing interests

The authors declare no competing interests.

Additional information

Supplementary Information The online version contains supplementary material available at <https://doi.org/10.1038/s41598-024-70016-2>.

Correspondence and requests for materials should be addressed to D.K.

Reprints and permissions information is available at www.nature.com/reprints.

Publisher's note Springer Nature remains neutral with regard to jurisdictional claims in published maps and institutional affiliations.

Open Access This article is licensed under a Creative Commons Attribution-NonCommercial-NoDerivatives 4.0 International License, which permits any non-commercial use, sharing, distribution and reproduction in any medium or format, as long as you give appropriate credit to the original author(s) and the source, provide a link to the Creative Commons licence, and indicate if you modified the licensed material. You do not have permission under this licence to share adapted material derived from this article or parts of it. The images or other third party material in this article are included in the article's Creative Commons licence, unless indicated otherwise in a credit line to the material. If material is not included in the article's Creative Commons licence and your intended use is not permitted by statutory regulation or exceeds the permitted use, you will need to obtain permission directly from the copyright holder. To view a copy of this licence, visit <http://creativecommons.org/licenses/by-nc-nd/4.0/>.

© The Author(s) 2024